TCABSE-J Research Article

ISSN: 2583- 2557, *Volume 1, Issue 5, pp20-25. 2023.*

TCABSE-J Interdisciplinary Sciences Journal

Solvent-guided quantitative structure-activity relationship (SG-QSAR): *In silico* SG-QSAR-based improvement of the human uridine phosphorylase-2 inhibitor binding affinity with potential applications in reducing the toxicity of chemotherapy

Abhinav V. K. S. Grandhi[1, 2], Madhumita Aggunna[1] and Ravikiran S. Yedidi[1, 3, *]

[1]Department of Intramural research core, The Center for Advanced-Applied Biological Sciences & Entrepreneurship (TCABS-E), Visakhapatnam 530016, A.P. India; [2]Koringa College of Pharmacy, Korangi 533461, A. P. India; [3]Department of Zoology, Andhra University, Visakhapatnam 530003, A.P. India. (*Correspondence to R.S.Y.: tcabse.india@gmail.com)

Keywords: Solvent mapping, QSAR, human uridine phosphorylase-2, 5-fluorouracil, uridine, uracil, cancer, cytotoxicity.

***In silico* drug discovery protocols typically include structure-based, fragment-based, quantitative structure-activity relationship (QSAR) studies, crystallographic solvent mapping, etc. In this study we combined the QSAR studies guided by the conserved crystallographic water molecules in the active site of human uridine phosphorylase-2 (hUPP-2) using the hUPP-2 receptor taken from PDB ID: 3P0F. The pre-existing inhibitor (5-benzylacyclouridine) complexed with hUPP-2 in this structure was taken as the starting lead compound (AG01001). Our current solvent-guided QSAR (SG-QSAR) studies systematically replaced the four conserved water molecules in the active site of hUPP2, one at a time, while optimizing the structure of AG01001 simultaneously. We were successful in improving the binding affinity of AG01001 from -8.0 kcal/mol. to -9.7 kcal/mol. The final SG-QSAR optimized compound (AG01056), although showed an improvement in its binding affinity in the absence of conserved waters (-9.7 kcal/mol.), showed a significant decrease in its binding affinity in the presence of conserved waters (-6.7 kcal/mol.) suggesting that AG01056 is indeed SG-QSAR optimized. AG01056 will be synthesized and evaluated in the future for its *in vitro* inhibitory activity.**

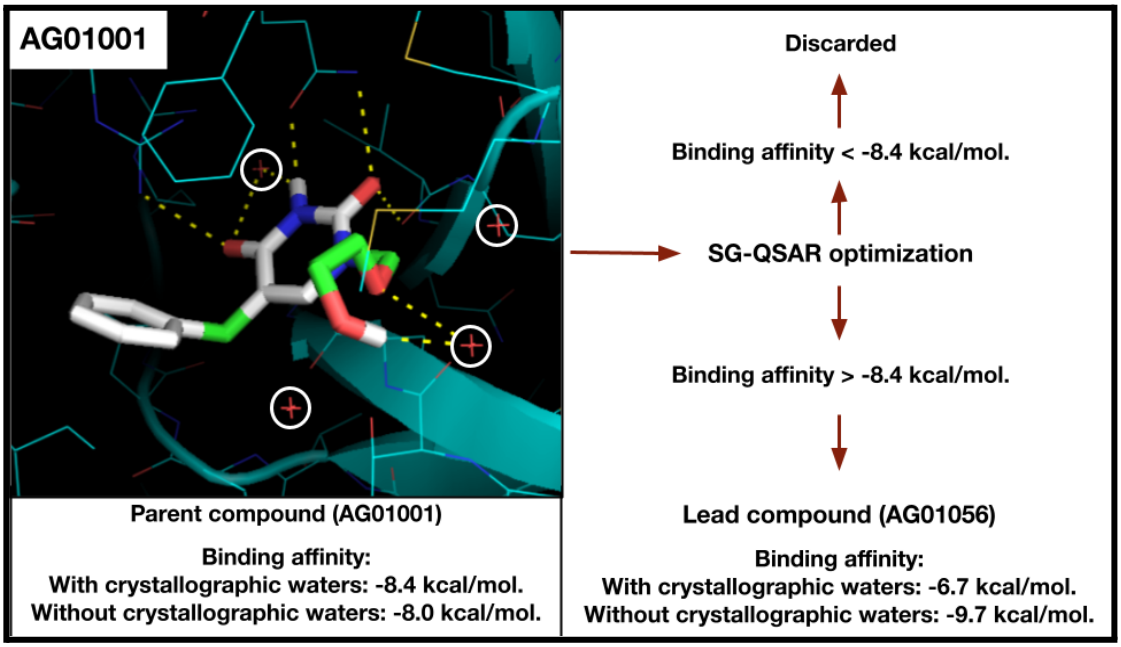

Graphical abstract: The structure of (AG01001) from PDB ID: 3P0F was optimized using the solvent molecules in the binding site using SG-QSAR to obtain the final optimized compound (AG01056).

Citation: Grandhi, A.V.K.S., Aggunna, M., and Yedidi, R.S. (2023). Solvent-guided quantitative structure-activity relationship (SG-QSAR): *In silico* SG-QSAR- based improvement of the human uridine phosphorylase-2 inhibitor binding affinity with potential applications in reducing the toxicity of chemotherapy. *TCABSE-J*, Vol. 1, Issue 5:20-25. Epub: Mar 12th, 2023.

Cancer is still one of the leading causes for human morbidity worldwide with 10 million deaths in the year 2020 according to the World Health Organization (WHO). The cancers pertaining to breast, lung, prostate, gastric, skin, colon and rectum were listed among the most frequent [1]. Most often the chemotherapy (CTX) involving a cocktail of various anti-cancer drugs (ACDs) [2] is used as the first line of defense. Typically the ACDs include DNA damaging/alkylating agents such as cisplatin [3], cytotoxic antibiotics such as doxorubicin [4], antimetabolites such as antifolates (methotrexate) [5], purine analogs (mercaptopurine) [6], pyrimidine analogs (fluorouracil) [7], innate immunity boosters such as recombinant interferon gamma [8], histone deacetylase enzyme inhibitors such as belinostat [9], antiandrogens such as flutamide [10], antiestrogens such as tamoxifen [11], monoclonal antibodies (rituximab) [12], protein kinase inhibitors (imatinib) [13], natural products from plants such as taxanes (paclitaxel) [14], vinca alkaloids such vin-blastine) [15], topoisomerase inhibitors such as etoposide [16] and other agents such as pomalidomide [17], etc. Usage of pyrimidine analogs in CTX such as 5'-fluorouracil (5FU) and capecitabine (prodrug containing 5FU) primarily involves the uridine and thymidine starvation of cells due to low levels of uridine and thymidine [18]. This leads to decreased levels of DNA synthesis and/or replication and dysfunctional RNA molecules in the tumor cells which ultimately triggers apoptosis [19]. Most of the ACDs in CTX rely on this cellular apoptotic phenomenon. The 5FU is known to cause liver injury [20] due to toxic intermediate metabolites that may cause inhibition of mitochondrial function [21] and other issues such as neuronal disorders [22]. The 5FU and capecitabine are activated by the human uridine phosphorylase-2 (hUPP-2). Inhibition of hUPP-2 has been shown to have modulatory effects on the toxicology of 5FU/ capecitabine by raising the cellular uridine levels [23]. It has been previously shown that 5-benzyl acyclouridine (BAU) inhibits hUPP-2 with nanomolar potency (K_i: 98 nM [24]). The X-ray crystal structure of hUPP-2 in complex with BAU has been previously published with PDB ID: 3P0F [25]. Our recent structural analysis of hUPP-2 in complex with the BAU revealed at least four conserved crystallographic water molecules. In this study, we hypothesized that the binding affinity of BAU can be increased by redesigning BAU taking advantage of the 4 conserved waters in the active site of the hUPP-2. Accordingly, we performed a systematic solvent-guided quantitative structure-activity relationship (SG-QSAR) analysis study on BAU.

Materials & Methods:

Designing BAU analogs: Chemsketch software was used to prepare the 2D all the structures of BAU (AG01001) analogs.

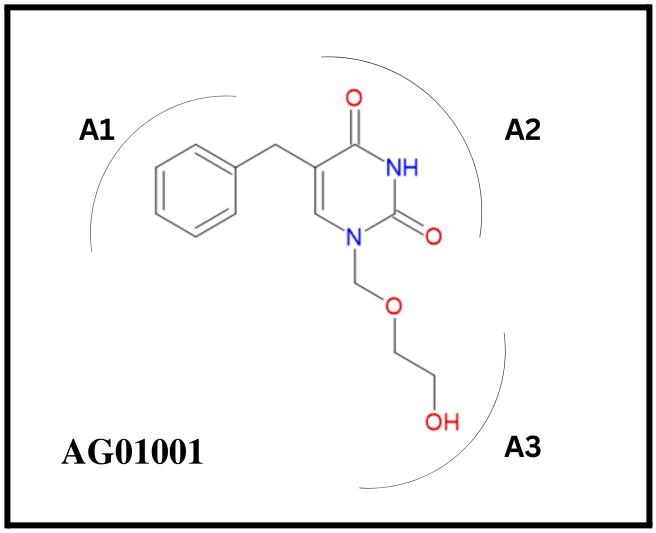

Figure 1. Two-dimensional structure of 5-bezylacyclouridine (BAU). This diagram was generated using ChemSketch software from ACD Labs.

Chemsketch was also used to generate the molecular weight, log P, log D, pKa values etc. for the analogs in the study. Chemsketch 3D view was used for generating the 3D conformers of each analog.

Preparation of the receptor: The 3D-structure of the hUPP2 in an inactive conformation with the bound 5-benzylacyclouridine (PDB-ID: 3P0F) was downloaded from the protein data bank (https://www.rcsb.org) and was analyzed using the PyMOL software. The protein-drug complex along with their interactions was saved for further analysis. The chain-A along with the four water molecules were saved as a protein molecule that served as the docking receptor. The receptor was further converted from .pdb format to .pdbqt file format using AutoDock Tools molecular graphics. The final receptor.pdbqt file was used to generate the docking grid.

Preparation of docking grid: The macromolecule (receptor) is taken to set the grid (a virtual box of dimensions that is set to cover the active site of the macromolecule, containing the area of the small molecule binding site and the obtained points of the dimensions and the center is used to create a configuration text file that is given to the Autodock Vina to read the file for extracting the binding affinities of different poses of each analog of the small molecule (ligand) [26]. The version 1.5.7 of Autodock tools is used to set the protein structure molecule from the 3P0F is used to adjust the grid to 10, 8 and 12 for X-dimension, Y-dimension and Z-dimension respectively. The 3-D center of the grid is taken as 14.128, -1.754 & 58.337 (x-center, y-center & z-center respectively).

ISSN: 2583- 2557, *Volume 1, Issue 5, pp20-25. 2023.*

TCABSE-J Interdisciplinary Sciences Journal

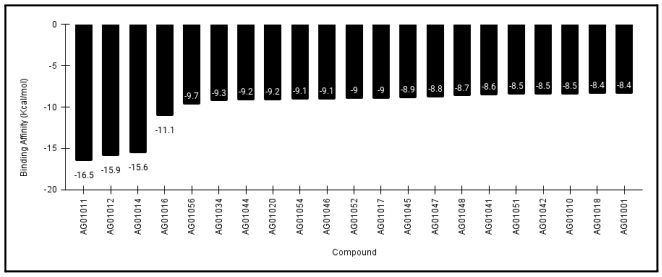

Figure 2. Analogs with binding affinity greater than AG01001.

The rotatable and non-rotatable bonds of each of the analogs are adjusted and saved as .pdbqt file formats. The files are saved in the .pdbqt formats for the AutoDock Vina to recognise and read the file for obtaining the binding affinities. AutoDock Vina produces the table of possible binding affinities by changing its modes of each analog (the binding pose of the drug molecule varies). The highest binding affinity is considered in each case. Analog AG010056 has the highest binding affinity of -9.7 kcal/mol while the parent drug (AG01001) has the binding affinity of -8.4 kcal/mol.

Molecular docking: The parent drug (AG01001) was re-docked using Vina software [27] as a positive control and subsequently all the analogs were docked using the same grid one at a time. Each of the PDBQT files of the analogs are used to compile in the configuration files. The configuration file helps Autodock Vina to read the files and compile which calculates the binding affinities. The command **"--config conf.txt --log log.txt"** helps the Autodock Vina to read the configuration file and write the log file (which is also a text file that gets automatically created after Vina finishes its run). Autodock Vina creates a possible number of poses of each analog, based on the evaluation of each binding pose with respect to the hUPP2 (receptor/protein); the best one with the best binding pose was considered for log-p values.

Structural analysis: The output files of each analog with the possible binding poses were evaluated using the PyMOL software and all the analogs are found with the better in the first binding pose. The molecular weights and the Log-P values of all the analogs were calculated using the Chemsketch software. Polar contacts were calculated in PyMOL and were considered only if they were relevant to that particular binding pose. Other binding poses showing non-selective binding and/or non-selective hydrogen bonds were discarded.

Results and Discussion:

In silico QSAR of the analogs: The binding affinities of all the tested analogs are summarized in Figure 2 and Figure 3.

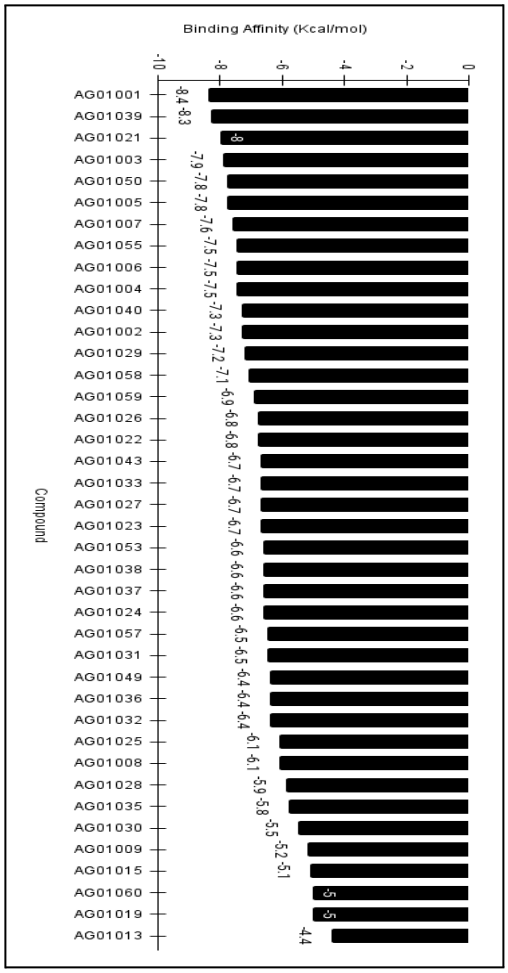

Figure 3. Analogs with binding affinity less than AG01001.

As shown in Table S1, the minimum (-4.4 kcal/mol.) and maximum (-16.5 kcal/mol.) binding affinities were obtained for the analogs AG01013 & AG01011, respectively, compared to the parent AG01001. As shown in Figure 2, the analogs, AG01011, AG01012, AG01014 and AG01016 showed significantly higher binding affinities compared to the parent compound, AG01001. As shown in Figure 3, AG01013 showed the least binding affinity among the 60 analogs that were built and tested in this study. Analogs with binding affinity values less than that of the parent compound were discarded irrespective of their binding poses. Similarly, analogs with binding affinity values greater than that of the parent compound were only considered for further analysis if their binding poses were similar to the parent compound. Hence the analog, AG01056 was considered as the lead molecule even though its binding affinity was far less than AG01011. Upon checking the binding pose and the corresponding binding affinity value, we further evaluate the binding profiles with polar contacts.

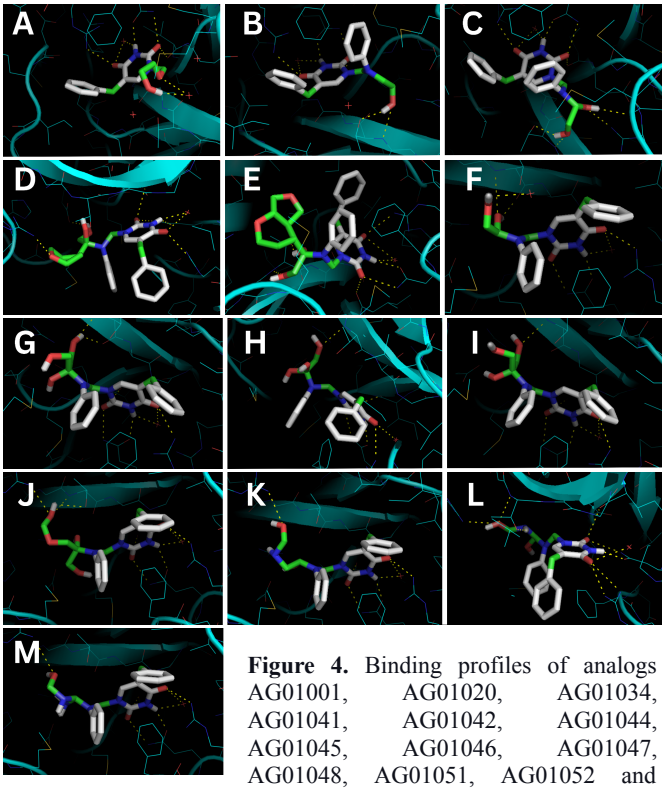

Figure 4. Binding profiles of analogs AG01001, AG01020, AG01034, AG01041, AG01042, AG01044, AG01045, AG01046, AG01047, AG01048, AG01051, AG01052 and AG01054 are shown in panels A to M, respectively. All analogs show multiple hydrogen bonds in the active site that are comparable to the parent compound, AG01001.

Evaluation of the binding profiles: The binding profiles including the hydrogen bonds, van der Waals contacts, etc. were analyzed for a total of 13 compounds including the parent (AG01001). As shown in Figure 4, all the 12 analogs showed hydrogen bonding within the active site with the key amino acid residues similar to AG01001 (Table 1). However, the binding profile for AG01056 will be published elsewhere and hence it is not displayed in Figure 4. Overall, these binding profiles support their corresponding binding affinities in comparison to the parent compound suggesting that the SG-QSAR is a better way of lead optimization rather than simple *in silico* QSAR studies.

Solvent guidance: The four conserved crystallographic water molecules that were chosen within a radius of 5 Å from the original compound, BAU were successfully used in the current solvent guided QSAR. During this process we added an additional benzene ring to the compound (Figure 4, panel B) that acted as a strong anchor for the compound while the solvent mapping was explored. Analogs with extremely high binding affinity values were not considered in this study as they were designed strictly based on the solvent molecules ignoring the binding orientation of the parent molecule, AG01001.

Analog	Receptor	No.of H-Bonds
AG01001	0Δ	8
AG01020	2Δ	8
AG01034	3Δ	10
AG01041	3Δ	11
AG01042	3Δ	11
AG01044	2Δ	9
AG01045	3Δ	13
AG01046	3Δ	13
AG01047	3Δ	7
AG01048	3Δ	9
AG01051	3Δ	7
AG01052	3Δ	9
AG01054	3Δ	7
AG01056	3Δ	8

Table 1. Number of hydrogen bonds made by each one of the analogs displayed in Figure 4. The receptor may have none of the waters deleted (0Δ) or two waters deleted (2Δ) or three waters deleted (3Δ).

Compound	1Δ	2Δ	3Δ	4Δ	0Δ
AG01001	-8.1	-8.4	-8.2	-8.1	-8
AG01020	-8.9	-9.2	-9	-8.9	-6.9
AG01021	-8.7	-7.7	-8.7	-8	-6.7
AG01034	-9.1	-9.2	-9.3	-9	-7.1
AG01039	-6.8	-5.6	-8.3	-8.3	-4.8
AG01041	-6.3	-5.7	-8.6	-8.6	-3.5
AG01042	-3.7	-2.5	-8.5	-6.8	-4.4
AG01044	-9.1	-9.2	-8.4	-9	-7.5
AG01056	-9.5	-9.6	-9.7	-9.7	-6.7

Table 2. Binding affinities of selected analogs against receptors containing 3 (1Δ), 2 (2Δ), 1 (3Δ), 0 (4Δ) and 4 (0Δ) conserved water molecules in their active site.

However, these compounds will be considered further in a future study. As shown in Table 2, the active site waters were systematically replaced with a parallel QSAR of the parent compound, AG01001 that resulted either in an increase or decrease in the overall binding affinity of the analog. Hence we only considered those analogs that follow the binding orientation and hydrogen bonding pattern of the parent compound in this study. Evidently from Table 1, AG01056 is the only analog that showed a systematic increase in the binding affinity replacing the active site waters and a sudden drop in the binding affinity in the presence of all four waters. This trend was not clearly seen for any of the other analogs listed in Table 1 thus making AG01056 the lead molecule obtained through SG-QSAR.

Pharmacological properties of analogs: The BAU analogs evaluated in this article have altered properties such as an increase in the molecular weight or change in the predicted LogP values that may affect their pharmacological properties such as the bioavailability and ADME-T (absorption, distribution, metabolism, excretion and toxicity). However, the increase in molecular weight is not significantly high even though some analogs violate Lipinski's rule of five. These details can be understood only after the synthesis and evaluation of these analogs in future.

Conclusion:

The current study successfully explored the conserved crystallographic water molecules in the active site of the hUPP-2 by taking the PDB ID: 3P0F as the starting structure. Four conserved water molecules were identified (highlighted with white circles in the graphical abstract of this article) that were systematically replaced along with the QSAR of BAU. The new analog, AG01056 identified in this study has potential implications in combination chemotherapy where one could reduce the toxic effects of 5-FU, Capecitabine, etc. This analog will be synthesized and evaluated in future.

Acknowledgements: We thank The Yedidi Institute of Discovery and Education, Toronto for scientific collaborations.

Conflict of interest: The authors declare no conflict of interest in this study. However, this research article is an ongoing project currently at TCABS-E, Visakhapatnam, India.

Author contributions: A.G. and M.A. performed Bioinformatics analysis and docking studies including the identification of binding poses for BAU analogs. R.S.Y. is the principal investigator who designed the project, trained both G.V.K.S.A. and M.A. in Bioinformatics, docking and *in vitro* experiments, secured required material for the project, provided the laboratory space and computational facilities needed, wrote and edited the manuscript.

References

1. The World Health Organization (WHO) Cancer key facts https://Cancer (who.int)/news-room/fact-sheets/detail/cancer.
2. LiverTox: Clinical and Research Information on Drug-Induced Liver Injury [Internet]. Bethesda (MD): National Institute of Diabetes and Digestive and Kidney Diseases; 2012-. Antineoplastic Agents. [Updated 2022 Sep 1]. Available from: https://www.ncbi.nlm.nih.gov/books/NBK548022/.
3. Ghosh S. Cisplatin: The first metal based anticancer drug. *Bioorg Chem*. 2019; 88:102925. doi:10.1016/j.bioorg.2019.102925.
4. Rivankar S. An overview of doxorubicin formulations in cancer therapy. *J Cancer Res Ther*. 2014;10(4):853-858. doi: 10.4103/0973-1482.139267.
5. Puig L. Methotrexate: new therapeutic approaches. *Actas Dermosifiliogr*. 2014; 105(6): 583-589. doi:10.1016/j.ad.2012.11.017.
6. Elgemeie GH. Thioguanine, mercaptopurine: their analogs and nucleosides as antimetabolites. *Curr Pharm Des*. 2003;9(31):2627-2642. doi:10.2174/1381612033453677.
7. Diasio RB, Harris BE. Clinical pharmacology of 5-fluorouracil. *Clin Pharmacokinet*. 1989;16(4):215-237. doi:10.2165/00003088-198916040-00002.
8. Castro F, Cardoso AP, Gonçalves RM, Serre K, Oliveira MJ. Interferon-Gamma at the Crossroads of Tumor Immune Surveillance or Evasion. *Front Immunol*. 2018;9:847. Published 2018 May 4. doi:10.3389/fimmu.2018.00847.
9. O'Connor OA, Horwitz S, Masszi T, et al. Belinostat in Patients With Relapsed or Refractory Peripheral T-Cell Lymphoma: Results of the Pivotal Phase II BELIEF (CLN-19) Study. *J Clin Oncol*. 2015;33(23):2492-2499. doi:10.1200/JCO.2014.59.2782.
10. Giorgetti R, di Muzio M, Giorgetti A, Girolami D, Borgia L, Tagliabracci A. Flutamide-induced hepatotoxicity: ethical and scientific issues. *Eur Rev Med Pharmacol Sci*. 2017;21(1 Suppl):69-77.
11. Jordan VC. Tamoxifen: a most unlikely pioneering medicine. *Nat Rev Drug Discov*. 2003;2(3):205-213. doi:10.1038/nrd1031.
12. Salles G, Barrett M, Foà R, et al. Rituximab in B-Cell Hematologic Malignancies: A Review of 20 Years of Clinical Experience. *Adv Ther*. 2017;34(10):2232-2273. doi:10.1007/s12325-017-0612-x.
13. Cohen P, Cross D, Jänne PA. Kinase drug discovery 20 years after imatinib: progress and future directions. *Nat Rev Drug Discov*. 2021;20(7):551-569. doi:10.1038/s41573-021-00195-4
14. Zhu L, Chen L. Progress in research on paclitaxel and tumor immunotherapy. *Cell Mol Biol Lett*. 2019;24:40. Published 2019 Jun 13. doi:10.1186/s11658-019-0164-y.
15. Radakovic A, Boger DL. Ultra-potent vinblastine analogues improve on-target activity of the parent microtubulin-targeting compound. *Bioorg Med Chem Lett*. 2019;29(11):1370-1374. doi:10.1016/j.bmcl.2019.03.036.
16. Hande KR. Etoposide: four decades of development of a topoisomerase II inhibitor. *Eur J Cancer*. 1998;34(10):1514-1521. doi:10.1016/s0959-8049(98)00228-7.
17. Zhu YX, Kortuem KM, Stewart AK. Molecular mechanism of action of immune-modulatory drugs thalidomide, lenalidomide and pomalidomide in multiple myeloma. *Leuk Lymphoma*. 2013;54(4):683-687. doi:10.3109/10428194.2012.728597.
18. Longley DB, Harkin DP, Johnston PG. 5-fluorouracil: mechanisms of action and clinical strategies. *Nat Rev Cancer*. 2003;3(5):330-338. doi:10.1038/nrc1074
19. Makin G, Hickman JA. Apoptosis and cancer chemotherapy. *Cell Tissue Res*. 2000;301(1):143-152. doi:10.1007/s004419900160.
20. Vestfrid MA, Castelleto L, Giménez PO. Necrósis hepática difusa en el tratamiento con 5-fluorouracilo [Diffuse liver necrosis in treatment with 5-fluorouracil]. *Rev Clin Esp*. 1972; 125 (6):549-550.
21. Di Federico A, Nuvola G, Sisi M, Lenzi B, Nobili E, Campana

D. Hyperammonemic encephalopathy during XELOX regimen. Is it capecitabine or oxaliplatin responsible?. *Anticancer Drugs*. 2020;31(10):1103-1105. doi:10.1097/CAD.0000000000000987.

22. Yeh KH, Cheng AL. High-dose 5-fluorouracil infusional therapy is associated with hyperammonaemia, lactic acidosis and encephalopathy. *Br J Cancer*. 1997;75(3):464-465. doi:10.1038/bjc.1997.79.
23. Chu MY, Naguib FN, Iltzsch MH, et al. Potentiation of 5-fluoro-2'-deoxyuridine antineoplastic activity by the uridine phosphorylase inhibitors benzylacyclouridine and benzyloxybenzylacyclouridine. *Cancer Res*. 1984;44(5): 1852-1856.
24. Niedzwicki JG, Chu SH, el Kouni MH, Rowe EC, Cha S. 5-benzylacyclouridine and 5-benzyloxybenzylacyclouridine, potent inhibitors of uridine phosphorylase. *Biochem Pharmacol*. 1982;31(10):1857-1861. doi:10.1016/0006-2952(82)90488-9.
25. Roosild TP, Castronovo S, Villoso A, Ziemba A, Pizzorno G. A novel structural mechanism for redox regulation of uridine phosphorylase 2 activity. *J Struct Biol*. 2011;176(2):229-237. doi:10.1016/j.jsb.2011.08.002.
26. Aggunna and Yedidi (2022). In silico quantitative structure-activity relationship analysis of a highly potent experimental HIV-1 protease inhibitor, GRL10413. *TCABSE-J*, 2022; 1(3):10-17.
27. Trott O, Olson AJ. AutoDock Vina: improving the speed and accuracy of docking with a new scoring function, efficient optimization, and multithreading. *J Comput Chem*. 2010;31(2): 455-461. doi: 10.1002/jcc.21334.
28. Yasuno, H., Kurasawa, M., Yanagisawa, M., Sato, Y., Harada, N., & Mori, K. (2013). Predictive markers of capecitabine sensitivity identified from the expression profile of pyrimidine nucleoside-metabolizing enzymes. Oncology Reports, 29, 451-458. https://doi.org/10.3892/or.2012.2149.

Full Figure Legends:

Figure 1. Two-dimensional structure of 5-bezylacyclouridine (BAU) along with its binding orientations into the receptor binding pockets, A1, A2 and A3 taken from the PDB ID: 3P0F. This diagram was generated using ChemSketch software from ACD Labs.

Figure 2. Analogs with binding affinity greater than the parent compound, AG01001. A total of 20 compounds were identified with their binding affinity values ranging between -8.4 kcal/mol. and -16.5 kcal/mol.

Figure 3. Analog with binding affinities lower than the parent compound, AG01001. A total of 39 compounds were identified with their binding affinity values ranging between -8.4 kcal/mol. and -4.4 kcal/mol.

Figure 4. Binding profiles of analogs AG01001, AG01020, AG01034, AG01041, AG01042, AG01044, AG01045, AG01046, AG01047, AG01048, AG01051, AG01052 and AG01054 are shown in panels A to M, respectively. All analogs show multiple hydrogen bonds in the active site that are comparable to the parent compound, AG01001. The heterocyclic ring that forms the uridine base is constantly engaged in three hydrogen bonds in all panels which was one of the criteria that was implied in choosing the lead molecule.